Solution structure of Pi4, a short four-disulfide-bridged scorpion toxin specific of potassium channels.

J. Iñaki Guijarro, Sarrah M'Barek, Froylan Gómez-Lagunas, Damien Garnier, Hervé Rochat, Jean-Marc Sabatier, Lourival D. Possani, Muriel Delepierre, Lourrival Possani

Solution structure of Pi4, a short four-disulfide-bridged scorpion toxin specific of potassium channels

J. IÑAKI GUIJARRO,[1] SARRAH M'BAREK,[2] FROYLAN GÓMEZ-LAGUNAS,[3] DAMIEN GARNIER,[1] HERVÉ ROCHAT,[2] JEAN-MARC SABATIER,[2] LOURRIVAL D. POSSANI,[4] AND MURIEL DELEPIERRE[1]

[1]Unité de RMN des Biomolécules (CNRS URA 2185), Dépt. de Biologie Structurale et Chimie, Institut Pasteur, 75724 Paris Cedex 15, France
[2]Laboratoire de Biochimie CNRS UMR 6560, and Laboratoire International Associé d'Ingéniérie Biomoléculaire, Faculté de Médecine Nord, 13916 Marseille Cedex 20, France
[3]Department of Physiology, School of Medicine, National Autonomous University of Mexico, D.F. 04510 Mexico
[4]Department of Molecular Medicine and Bioprocesses, Institute of Biotechnology, National Autonomous University of Mexico, Cuernavaca 62210 Mexico

(RECEIVED May 6, 2003; FINAL REVISION June 10, 2003; ACCEPTED June 13, 2003)

Abstract

Pi4 is a short toxin found at very low abundance in the venom of *Pandinus imperator* scorpions. It is a potent blocker of K^+ channels. Like the other members of the α-KTX6 subfamily to which it belongs, it is cross-linked by four disulfide bonds. The synthetic analog (sPi4) and the natural toxin (nPi4) have been obtained by solid-phase synthesis or from scorpion venom, respectively. Analysis of two-dimensional ^1H NMR spectra of nPi4 and sPi4 indicates that both peptides have the same structure. Moreover, electrophysiological recordings of the blocking of Shaker B K^+ channels by sPi4 (K_D = 8.5 nM) indicate that sPi4 has the same blocking activity of nPi4 (K_D = 8.0 nM), previously described. The disulfide bonds have been independently determined by NMR and structure calculations, and by Edman-degradation/mass-spectrometry identification of peptides obtained by proteolysis of nPi4. Both approaches indicate that the pairing of the half-cystines is ^6C–^{27}C, ^{12}C–^{32}C, ^{16}C–^{34}C, and ^{22}C–^{37}C. The structure of the toxin has been determined by using 705 constraints derived from NMR data on sPi4. The structure, which is well defined, shows the characteristic α/β scaffold of scorpion toxins. It is compared to the structure of the other α-KTX6 subfamily members and, in particular, to the structure of maurotoxin, which shows a different pattern of disulfide bridges despite its high degree of sequence identity (76%) with Pi4. The structure of Pi4 and the high amounts of synthetic peptide available, will enable the detailed analysis of the interaction of Pi4 with K^+ channels.

Keywords: Cysteine-stabilized αβ motif; disulfide bridges; NMR; *Pandinus imperator*; potassium channel; scorpion toxin

Supplemental material: See www.proteinscience.org.

Scorpion venoms are rich in basic polypeptides that alter the ion permeability of cellular membranes by interacting with ion channels. These polypeptides can recognize different types of Na^+, K^+, Ca^{2+}, or Cl^- channels and can be toxic for mammals, insects, or crustaceans. Because of the variety of toxins found in scorpion venoms, their usually high affinities, and their differences in specificity for channel types and subtypes, these small proteins constitute very useful tools for the characterization of ion channels and are widely used in neurobiology research. Although scorpion toxins can display large differences in sequence, activity, and

Reprint requests to: Muriel Delepierre, Unité de RMN des Biomolécules (CNRS URA 2185), Dépt. de Biologie Structurale et Chimie, Institut Pasteur, 28 rue du Docteur Roux, 75724 Paris Cedex 15, France; e-mail: murield@pasteur.fr; fax: 33-145688929.

Abbreviations: a.m.u., atomic mass unit; COSY, correlation spectroscopy; CSI, chemical shift index; DQF-COSY, double-quantum–filtered COSY; HPLC, high-performance liquid chromatography; MTX, maurotoxin; NOE, nuclear Overhauser effect; NOESY, nuclear Overhauser effect spectroscopy; nPi4, Pi4 purified from scorpion venom; Pi4, *Pandinus imperator* toxin 4; RMSD, root mean square deviation; sPi4, synthetic Pi4; TFA, trifluoroacetic acid; TOCSY, total correlation spectroscopy.

Article and publication are at http://www.proteinscience.org/cgi/doi/10.1110/ps.03186703.

specificity, these share a common scaffold stabilized by disulfide bridges and consisting of an α-helix and a double- or triple-stranded antiparallel β-sheet (Bontems et al. 1991). Understanding the mode of action of toxins, and in particular their differences in specificity, requires the fine characterization of their structures.

Toxins acting as K^+-channel inhibitors are short polypeptides, 23–47 residue long (Batista et al. 2000; Corona et al. 2002). To the exception of the members of the α-KTX6 subfamily, almost all of these toxins have six cysteines that form three disulfide bridges with the pairings C1–C4, C2–C5, and C3–C6. The disulfide bonds C2–C5 and C3–C6 link the α-helix to the second strand of the β-sheet, whereas the bridge C1–C4 links an N-terminal loop to the first strand of the β-sheet.

The five known members of the α-KTX6 subfamily contain four disulfide bonds (Fig. 1). These toxins have two additional cysteines, one (C4) between cysteines C3 and C4, and another (C8) C-terminal to cysteine C7 in three-disulfide–bridged toxins. Interestingly, two different arrangements of disulfides have been described for the members of this subfamily. Pi1 (Olamendi-Portugal et al. 1996), Pi7 (Olamendi-Portugal et al. 1998; Delepierre et al. 1999), and HsTX1 (Lebrun et al. 1997) show half-cystine pairings of the type C1–C5, C2–C6, C3–C7, and C4–C8. This arrangement of S–S bonds contains three disulfide bridges analogous to those observed for three disulfide toxins. The additional bond (C4–C8), which is formed by the two additional cysteines, links the loop between the α-helix and the first β-sheet strand to the C terminus. Maurotoxin (MTX) displays a different S–S bond topology: C1–C5, C2–C6, C3–C4, and C7–C8 (Kharrat et al. 1996, 1997). The different

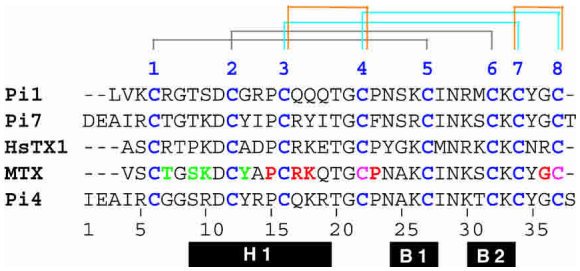

Figure 1. Sequence alignment of the αKTX6 subfamily. Cysteines are shown in blue. Solid lines represent disulfide-bridge pairings for standard (cyan), nonstandard (orange), and common to standard and nonstandard topologies (gray). MTX residues that have been mutated without any effect on its S–S bridge topology are labeled in green, and those that had an effect (change to standard topology) are colored in red (Fajloun et al. 2000c; Carlier et al. 2001). In magenta, two cysteine residues that have been mutated into α-aminobutyrate (Abu). The double Cys→Abu mutant adopts the standard arrangement of three-disulfide–bridged scorpion toxins (Fajloun et al. 2000b). Numbering corresponds to that of Pi4 and Pi7. The secondary structure of Pi4 as determined in this work is indicated by solid rectangles. (H indicates α-helix; B, β strand). The alignment was obtained with CLUSTAL W (Thompson et al. 1994).

S–S bonds in MTX (C3–C4, C7–C8) link contiguous regions in the sequence. For the sake of simplicity, these arrangements will be called, from here on, standard (Pi1, Pi7, and HsTX1) and nonstandard (MTX). Even though MTX has a nonstandard topology of S–S bonds, it displays the characteristic structure of scorpion toxins (Blanc et al. 1997). Several mutants of MTX have been synthesized, their S–S bond topology determined, their electrophysiology studied, and, for some of the mutants, their structure established by NMR (Fajloun et al. 2000b,c; Carlier et al. 2001). Mutation at several positions close to cysteines C3 and C4 resulted in a change from a nonstandard to a standard arrangement of S–S bonds, with, in general, only minor modifications on the activity and specificity of the mutants relative to wild-type MTX. The former result indicates that key positions in the sequence, close to cysteine residues C3 and C4 control the formation of S–S bonds (Fig. 1).

Pi4, a member of the α-KTX6 subfamily, shows a high level of identity with MTX (76% identity, 85% similarity) but displays some differences in sequence in the region close to cysteines C3 and C4. This toxin is found at low abundance in the venom of *Pandinus imperator* scorpions. It blocks Shaker B K^+ channels expressed in Sf9 insect cells (K_D = 8 nM), competes with the K^+-channel specific noxiustoxin for rat brain synaptosomal membranes (IC_{50} = 10 nM; Olamendi-Portugal et al. 1998), binds to small-conductance Ca^{2+}-activated SK channels, and is among the most potent known inhibitors (IC_{50} = 8 pM) of rat Kv1.2 channels (M'Barek et al. 2003). As a first step to study at an atomic level the interaction of this toxin with potassium channels to shed light on its mode of action and its specificity, we have solved its structure in solution by ^{1}H-NMR. Here, we describe the comparison by NMR, of Pi4 obtained from scorpion venom (nPi4, available only in small amounts) and by solid-state synthesis (sPi4), the determination of its disulfide bridges, its solution structure, and electrophysiological data of synthetic Pi4. A special attention was paid to the determination of disulfide bonds that were independently identified by NMR and by standard techniques of analysis of purified peptides derived from enzymatic cleavage.

Results

NMR assignments

^{1}H spectra of the natural (nPi4) and synthetic (sPi4) peptides were obtained at 293, 303, and 313 K in 5 mM sodium acetate buffer (pH 4.0), prepared in H_2O. sPi4 spectra were also recorded by using the same buffer prepared in D_2O. Except for proton $H\gamma_{12}$ from residue ^{28}I, all the resonances of nonlabile protons were assigned for both peptides under all the experimental conditions that were used. The resonances of all backbone and side chain amide protons, as

well as the proton signals of the guanidinium group of arginines and of the amino group of lysines, were also identified in spectra recorded by using H_2O solutions. NMR assignments obtained from data at 303 K are summarized in Tables A (sPi4 and nPi4, H_2O buffer) and B (sPi4, D_2O buffer) of the supplementary material.

Comparison of natural and synthetic Pi4 NMR data

NMR spectra can be thought of as fingerprints of a given structure. The pattern of cross-peaks in nuclear Overhauser effect spectroscopy (NOESY) spectra, which arise from dipolar interactions between protons that are close to each other (≤5 Å apart), is particularly sensitive to even small differences in structure. Purged correlation spectroscopy (COSY), total correlation spectroscopy (TOCSY) and NOESY spectra of synthetic Pi4 at 293, 303, and 313 K are very similar to the equivalent spectra of natural Pi4. In particular, except for a few signals that show significantly different amide proton chemical shifts, the NOESY spectra of both peptides are effectively identical (Fig. 2). Indeed, spectra superpose very well, if one allows for small variations in chemical shifts (≤0.03 ppm) and differences in sensitivity and in water-signal suppression. To the exception of the amide protons of residues 37 and 38, all the equivalent protons in nPi4 and sPi4 show the same chemical shift to within 0.03 ppm at the three temperatures used (see Supplemental Material, Table A). More specifically, the chemical shifts of all the α and β protons of Cys residues, which are expected to vary for different disulfide bridge arrangements, agree within experimental error. In addition, the temperature coefficients of the backbone amide protons of nPi4 and sPi4, which reflect hydrogen bonding and burial of HN protons, are also in agreement (Supplemental Material, Table C). Taken together, these results unambiguously demonstrate that the synthetic and natural Pi4 toxins have the same structure and, thereby, the same pattern of disulfides.

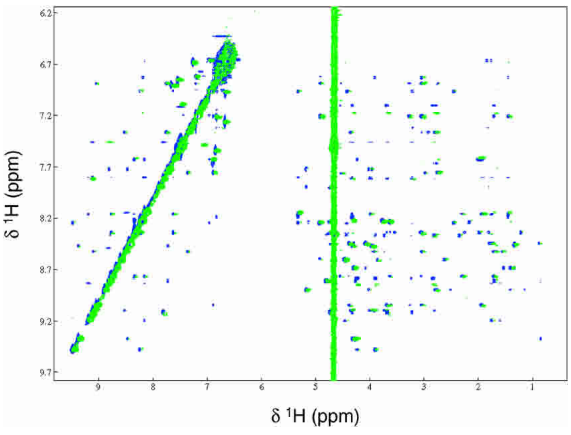

Figure 2. Superposition of a region of the NOESY spectra of Pi4 extracted from scorpion venom (green) and obtained by chemical synthesis (blue). Spectra were acquired at 303 K by using a mixing time of 200 msec.

sPi4 was synthesized with a carboxyl group (COO^-) at its C terminus. During the analysis of the NMR spectra of nPi4, however, we noticed that the natural toxin contains an amide group (COH_2N) at its C-terminal end. Indeed, in TOCSY and NOESY spectra of nPi4, there is a spin system that shows a single cross-peak between two exchangeable protons that resonate at 7.05 and 7.49 ppm (303 K), which are typical frequencies for H_2N amide protons. This spin system is absent in spectra of sPi4. Moreover, mass spectrometry analysis of nPi4 gave a molecular mass of 4178.4 atomic mass units (a.m.u.), closer to the amidated form (expected mass of 4178.9), than to the carboxylated form (expected mass of 4179.9). Because the absolute error of measurement is greater with bigger peptides, a sample of nPi4 was reduced, carboxymethylated, and digested with trypsin. The peptide eluting at 23.41 min on the high-performance liquid chromatography (HPLC) chromatogram (run in the same conditions described in Olamendi-Portugal et al. 1998) was sequenced by automatic Edman degradation to confirm the sequence C-Y-G-C-S, of the C-terminal peptide. The experimental molecular mass of this peptide was 647.1 a.m.u., which corresponds exactly to the theoretical value expected for the amidated peptide, unequivocally confirming the presence of a serine amide at the end of the peptide. Noteworthy, the different C terminus of nPi4 and sPi4 can account for the differences observed in their corresponding spectra, as only the HN protons of the C-terminal residue ^{38}S and of the neighboring ^{37}C display significantly different chemical shifts in nPi4 (8.85 and 8.46 ppm at 303 K, respectively) and sPi4 (8.79 and 8.36 ppm at 303 K, respectively). Despite the differences in chemical shift observed for these HN protons, these have very similar temperature coefficients (Supplemental Material, Table C), and the rest of the analogous protons of residues 37 and 38 present effectively the same resonance frequency. Hence, whether the C-terminal group is an amide (nPi4) or a carboxyl (sPi4) does not have any influence (not even locally) on the structure of Pi4. To summarize, NMR data indicates that synthetic Pi4 adopts the same structure and S–S pattern than the natural toxin.

Disulfide bridges

The disulfide bridge arrangement of Pi4 was first established by NMR and modeling using data obtained for sPi4 and the programs ARIA and CNS. Structure calculations were started from completely unassigned nuclear Overhauser effect (NOE; initial rate) data and ϕ angle constraints. Four different structure calculations were considered: a, no S–S bond constraint; b, ambiguous S–S bond constraints (Nilges 1995); c, standard S–S bonds (C1–C5, C2–C6, C3–C7, and C4–C8); and d, nonstandard MTX-like

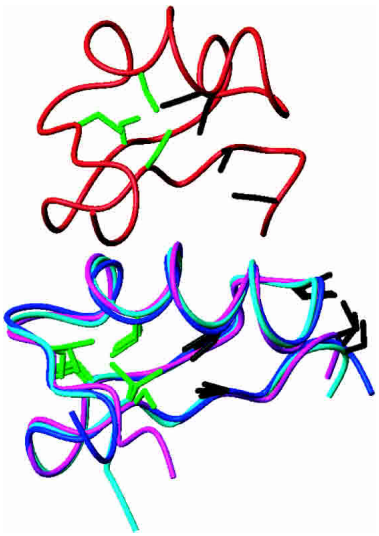

Figure 3. Pi4 disulfide-bridge assignment by NMR. Structures of Pi4 obtained with ARIA and CNS using no S–S constraint (magenta, structure a), ambiguous S–S constraints (cyan, structure b), and standard (blue, structure c) or nonstandard (red, structure d) disulfide topology are superimposed on backbone atoms between residues 4–37. The heavy atoms of side chains from Cys residues involved in S–S bridges that differ (black) or are common (green) to the standard and nonstandard S–S topologies are represented. The nonconvergent structure with nonstandard S–S arrangement is shifted upward for visualization purposes.

S–S bonds (C1–C5, C2–C6, C3–C4, and C7–C8). For each S–S pattern, 100 structures were calculated in the last iteration of ARIA, and the 10 lower energy structures were minimized in explicit water. Calculations without, with ambiguous, and with standard S–S bonds converge to the same structure and NOE assignments, whereas those performed with nonstandard S–S bonds generate a different structure (Fig. 3). Indeed, the backbone pairwise root mean square deviation (RMSD; residues 4–37) between structures a, b, and c varies between 0.45 and 0.6 Å, whereas that of structure d, obtained with nonstandard disulfides, shows an RMSD of ~2.5 Å with the others. In particular, the cysteine side chains superpose very well in structures a, b, and c, and the distances between Sγ atoms in these structures are in agreement with a standard S–S topology but not with a nonstandard one. Indeed, there is no short distance <4 Å between cysteines C3 and C4 or C7 and C8, which would be expected for a nonstandard S–S pattern. Moreover, there is at least one intercysteine NOE assigned to cysteine partners of standard S–S bridges, and importantly, there is no NOE assigned to interactions between C3–C4 or C7–C8. Contrastingly, in all the structures obtained considering the nonstandard cysteine pairing, there is a short distance between C3–C7, which is expected for a standard S–S pairing. Several additional arguments are in favor of a standard S–S pattern for Pi4. Indeed, the total (≤−890 versus −730 kcal/mole), Van der Waals (≤−50 versus −5 kcal/mole), and NOE (≤ 20 versus 40 kcal/mole) energies are substantially higher for the d structures; also, the latter show a significantly worse Ramachandran plot and a worse backbone conformation. Finally, structures calculated with nonstandard S–S bonds show a poor agreement with experimental data. For instance, although structures a, b, and c show a two-stranded antiparallel β-sheet, in accordance with $^3J_{HN}$ coupling constants, amide exchange data, amide temperature coefficients, and manual assignment of HN, Hα, and Hβ NOE connectivities, none of the structures calculated with nonstandard disulfide bridges displays the β-sheet. In conclusion, NMR data demonstrates that Pi4 adopts the standard pattern of disulfide bonds.

The S–S bonding pattern was also established for nPi4 by usual techniques of identification of purified peptides obtained after enzymatic cleavage of the natural protein. Several peptides were obtained from the enzymatic hydrolysis of nPi4 with trypsin and chymotrypsin as described in Materials and Methods. Hydrolysis was performed in slightly acidic conditions to avoid any rearrangement of disulfides. The peptides were analyzed by N-terminal sequencing and mass spectrometry. Although some undigested Pi4 was observed in the chromatogram, together with peptides showing partial hydrolysis and containing more than one disulfide pair, an important fraction of each of the expected fragments containing individual and unique disulfide pairs was obtained. The results are shown in Table 1. As it is sometimes difficult to identify the last pair of amino acids when automatic Edman degradation mass spectrometry was

Table 1. *Disulfide bridge determination by Edman degradation and mass spectrometry*

Retention time (min)	Amino acid sequence	Experimental mass	Theoretical mass
TC 14.22	$TG^{22}CPNAK$ | $G^{37}CS$	953.5	954.0
TC 17.56	$^{6}CGGSR$ | $^{27}CIN(K)$	953.5	954.1
TC 19.14	$D^{12}C(Y)$ | $T^{32}CK$	748.4	748.8
TC 20.19	$RP^{16}C(QK)$ | ^{34}CY	913.4	914.0

First column is HPLC elution position of peptides obtained by proteolytic cleavage. TC, which is followed by the retention time, indicates trypsin/chymotrypsin. Second column is amino acid sequence obtained by direct Edman degradation and, in parenthesis, residues identified by mass spectrometry. The sequences shown correspond to the segments of primary structure that are bound together through a disulfide bridge in the native peptide. The third and fourth columns correspond to the experimental molecular mass of each peptide as determined from the ion-trap mass spectrometer analysis or as expected from the sequence of Pi4 and the putative sites of cleavage of the hydrolytic enzymes, respectively.

used to complete the sequence of some peptides (amino acids in parenthesis in Table 1). Molecular mass differences between the peptides, identified by Edman degradation and mass spectrometry (second column of Table 1), and the expected peptides, are smaller than one mass unit. This observation supports the conclusion that the identified sequences are indeed the expected sequences, based on the known primary structure of Pi4 and the putative sites of cleavage of the enzymes that were used. Analysis of the results in Table 1 indicates that the disulfide bridges of nPi4 are formed between ^{6}C–^{27}C, ^{12}C–^{32}C, ^{16}C–^{34}C, and ^{22}C–^{37}C. Hence, in conclusion, both NMR and conventional techniques indicate that natural Pi4 and its synthetic analog adopt the standard arrangement of disulfide bridges.

Structure of Pi4

Synthetic Pi4 data were used for structure calculations as the synthetic toxin was available in much larger amounts than the toxin extracted from scorpion venom. The NOE data that characterize the secondary structure of proteins, $^{3}J_{HN}$ coupling constants, amide exchange data, amide temperature coefficients, and Hα chemical shift data are shown in Figure 4. Together, these data indicate that Pi4 displays an α-helix and a two-stranded β-sheet. The statistics of the family of 10 conformers calculated for Pi4 are summarized in Table 2. The structures were determined with a total of 679 meaningful distance constraints (642 unambiguous, 37 ambiguous), 16 dihedral angles, and 10 hydrogen bonds.

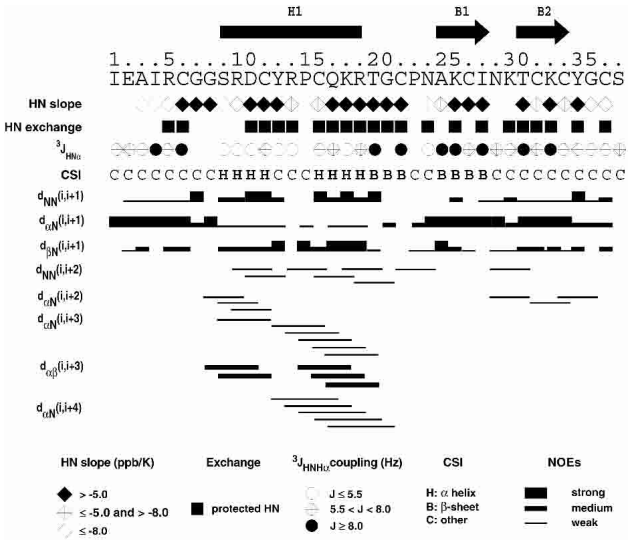

Figure 4. Summary of secondary structure NOE-related connectivities, amide exchange and temperature coefficient data, $^{3}J_{HN\text{-}H\alpha}$ coupling constants, and CSI (Wishart and Sykes 1994b) predictions. The secondary structure determined from the final structures is shown *above* the sequence: The helix H1 is represented by a rectangle, and the β-strands B1 and B2 by arrows.

Table 2. *Structural statistics for the ensemble of 10 conformers calculated for Pi4*

Parameter	Value
Constraints	
Number of unambiguous distance restraints	642
Intraresidue, | j–i | = 0	265
Sequential, | j–i | = 1	148
Medium range, 2 ≤ | j–i | ≤ 4	55
Long range, | j–i | > 5	174
Number of ambiguous distance restraints	37
Intraresidue, | j–i | = 0	9.2
Sequential, | j–i | = 1	11
Medium range, 2 ≤ | j–i | < 4	7.0
Long range, | j–i | ≥ 4	9.8
Total number of distance restraints[a]	679
Intraresidue, | j–i | = 0	274.2
Sequential, | j–i | = 1	159.0
Medium range, 2 ≤ | j–i | < 4	62.0
Long range, | j–i | ≥ 4	183.8
Number of dihedral ϕ angle restraints	16
Number of hydrogen bonds	10
Residual distance constraint violations	
Number ≥ 0.3 Å	0
Number ≥ 0.1 Å	5.7 ± 2.1
RMS from NOEs (Å)	0.017 ± 0.002
Residual dihedral angle constraint violations	
Number ≥ 5.0°	0
RMS from dihedrals (°)	0.5 ± 0.1
Energies (kcal/mole)	
Total	−1115 ± 34
Van der Waals	−116 ± 6
Electrostatic	−1258 ± 30
Mean pairwise RMSD (Å)	
Backbone atoms N, Cα, C′ (1–38)	0.83 ± 0.21
Heavy atoms (1–38)	1.27 ± 0.22
Backbone atoms N, Cα, C′ (4–37)[b]	0.37 ± 0.08
Heavy atoms (4–37)[b]	0.93 ± 0.15
Ensemble Ramachandran plot:	
Residues in most favored regions	79.0 ± 5.0%
Residues in additionally allowed regions	21.0 ± 5.0%

[a] Meaningful distance constraints used for structure calculations.
[b] Mean of the pairwise RMSD between residues 4 and 37.

This corresponds to an average of 18.6 constraints per residue. No violation ≤0.3 Å or ≤5° is observed for distance or angle constraints, respectively. The structures display good covalent geometry, and 100% of backbone ϕ and Ψ dihedrals are located in the most favored and allowed regions of the Ramachandran plot.

Pi4 shows the α/β scaffold common to scorpion toxins (Fig. 5). The α-helix, which presents a bend at the level of proline 15, runs between residues ^{10}R and ^{20}T. The antiparallel β-sheet is composed of two strands (^{25}A–^{28}I and ^{31}T–^{34}C) separated by a two-residue-long bend. The structures display a good convergence between residues 4–37, with a mean pairwise RMSD between these residues of 0.37 ± 0.08 Å and of 0.93 ± 0.15 Å for the backbone and the heavy atoms, respectively. The N- and C-terminal end of the struc-

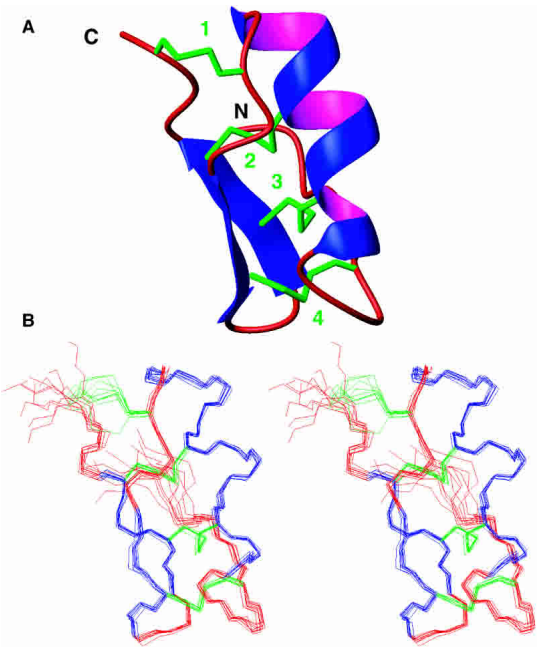

Figure 5. Solution structure of Pi4. (*A*) Ribbon diagram of the best conformer (lowest total energy). (*B*) Stereoview of the calculated family of 10 conformers. Secondary structures are shown in blue and the rest of the backbone in red. Bonds between side chain heavy atoms of cysteine residues as well as disulfide bonds are displayed in green.

tures are less well defined, which correlates with the low number of NOEs observed for residues ^{1}I, ^{2}E, and ^{38}S (Supplemental Material, Fig. A). This dispersion at both ends of the molecule most probably reflects the internal dynamics of the toxin. The three disulfides in common with three S–S bond toxins are well defined. The first disulfide (^{6}C–^{27}C) shows a right-handed conformation, whereas the second (^{12}C–^{32}C) and third (^{16}C–^{34}C) are left-handed. The cysteines involved in these disulfides are buried in the interior of the protein. As observed for HsTX1 (Savarin et al. 1999), the fourth disulfide (^{19}C–^{37}C) shows some variability, but most of the conformers have a left-handed disulfide. Cysteines ^{19}C and ^{37}C are partially exposed to the solvent. The hydrophobic core of Pi4 is mainly formed by the three buried cystines and residues ^{4}I, ^{13}Y, ^{15}P, ^{25}A, and ^{31}T. Residues ^{23}P and ^{17}Q also contribute to this core. Because Pi4 is a small protein, most residues are at least partially exposed to the solvent. Nevertheless, it is interesting to note that residues ^{26}K and ^{35}Y, which correspond to the so-called functional dyad residues and have been shown to be important for the interaction of other toxins with K^+ channels, are well exposed to the solvent.

Electrophysiological assays

To determine if sPi4 has the ability of the natural toxin to block Shaker B K^+ channels with high affinity, the effects of the synthetic peptide on these channels were tested by using the same expression system that had been used previously for assaying the natural toxin (Olamendi-Portugal et al. 1998). The left panel of Figure 6A shows control K^+ currents through Shaker B, evoked by 30-msec pulses from −30 to 60 mV in 10-mV increments, from a holding potential of −90 mV (see Materials and Methods). When sPi4 was added to the external solution at a concentration of 50 nM (Fig. 6A, middle), a clear reduction (~90% at all voltages) of the amplitude was obtained. The right panel shows that the effect was completely reversed after washing the cell with the control external solution. The above observations are summarized in Figure 6B that shows the I–V relationship of the traces in Figure 6A.

In the aim of determining the efficiency of blockage of sPi4 compared with nPi4, we measured its blocking effect as a function of peptide concentration (Fig. 6C). The blockage follows a sigmoidal curve with an equilibrium dissociation constant K_D of 8.5 nM. This value is basically identical to the value (8 nM) formerly obtained for nPi4 (Olamendi-Portugal et al. 1998), which demonstrates that sPi4 blocks Shaker B exactly in the same way than nPi4.

It is convenient to mention that although the results in Figure 6 were obtained with an external solution at pH 7.2, previous experiments with nPi4 were performed at pH 6.4 (Olamendi-Portugal et al. 1998). The remarkable similarity of the K_D values shows that in this range, the extracellular pH does not affect the binding of the toxin to the channels. This is in agreement with previous data obtained with other scorpion toxins (Gómez-Lagunas et al. 1997).

Discussion

Pi4 represents only ~0.5% of the soluble scorpion venom (Olamendi-Portugal et al. 1998). To obtain a well-defined structure and to study in detail the interaction of Pi4 with different subtypes of channels, high amounts of material are required. Hence, the molecule was obtained by chemical synthesis and in vitro oxidative folding, and compared with the peptide purified from venom. To the best of our knowledge, this is the first example in which a natural toxin and its synthetic or recombinant analog are compared at both the structural and functional levels. The comparison of several NMR spectra obtained at three different temperatures indicates that natural and synthetic Pi4 have the same structure, and thereby, the same S–S topology. Moreover, binding experiments on Shaker B K^+ channels expressed in insect cells indicate that sPi4 (K_D = 8.5 nM) has effectively the same activity toward these channels than nPi4 (K_D = 8 nM; Olamendi-Portugal et al. 1998). Thus, the disulfide-rich sPi4 is able to fold in vitro into the native conformation. During the analysis of the NMR experiments, we noticed that nPi4 is amidated on its C terminus, a result that was later confirmed by mass spectrometry. The synthetic pep-

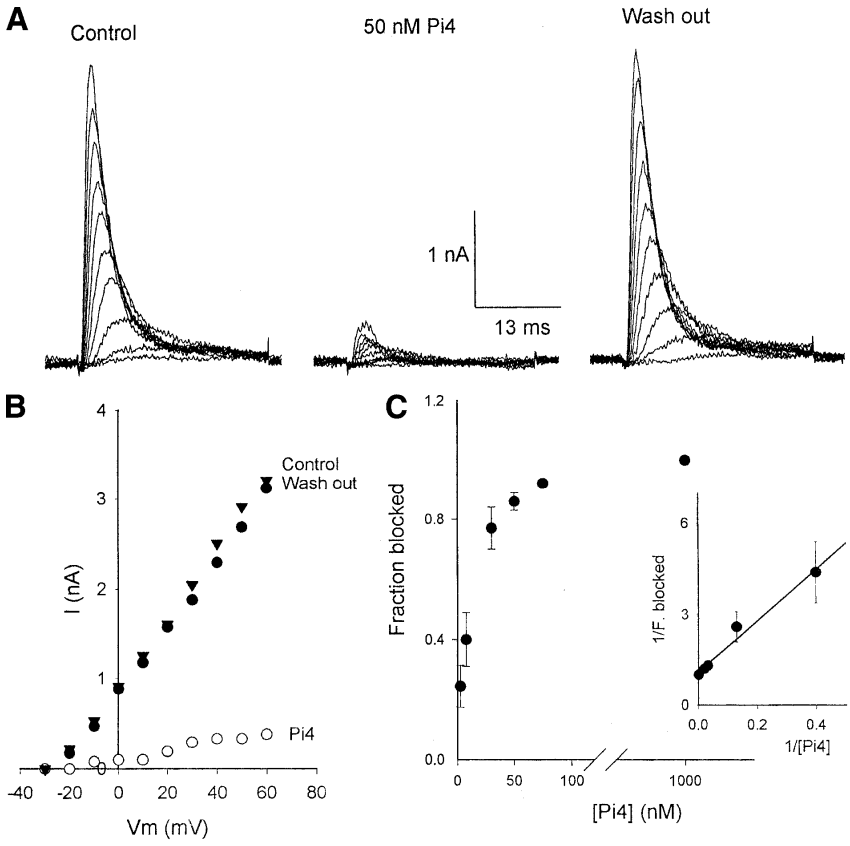

Figure 6. Synthetic Pi4 blocks Shaker B K^+ channels with high affinity. (*A*, *left*) K^+ currents through Shaker B channels evoked by 30-msec pulses from −30 to 60 mV. (*Center*) Residual K^+ currents in the presence of 50 nM sPi4 in the external solution. (*Right*) K^+ current recovery after washing the cell with the control external solution. (*B*) I–V relationship of the traces in *A*. (*C*) Fraction blocked as a function of [sPi4]. Fraction blocked = $1-(I/I_0)$, where I is the peak current in the presence of the indicated [sPi4], and I_0 is the control current, like in panel *A*. (*Inset*) The double reciprocal plot. The line corresponds to the least-squares fit of the points (K_D = 8.5 nM, r = 0.988). Holding potential = −90 mV. The internal solution was (in mM) 90 KF, 30 KCl, 2 $MgCl_2$, 10 EGTA, and 10 HEPES-K (pH 7.2), whereas the external solution was (in mM) 145 NaCl, 10 $CaCl_2$, and 10 HEPES-Na (pH 7.2).

tide, however, had previously been synthesized with a COO^- C-terminal group. That nPi4 and sPi4 show the same binding characteristics to Shaker B channels indicates that the C terminus is not implicated in binding to this channels. This is a relevant result because it has been observed for other toxins that replacement of a neutral amide group by a negative carboxyl function is deleterious for channel binding, and that residues close to the C terminus are often implicated in channel recognition (Sabatier et al. 1993; Devaux et al. 1995).

In standard techniques used for the determination of disulfide bonds, the protein is proteolyzed, very often for several hours at neutral or basic pH. During proteolysis, rearrangement of S–S bonds can in principle occur and lead either to an erroneous determination of disulfides or just hamper their determination (for an example of the latter with a scorpion toxin, see Lebrun et al. 1997). Protease refractory proteins or proteins with particular sequences may also pose a difficult problem to solve. To ensure that the S–S pairing of Pi4 would be established correctly, the latter was determined independently by NMR and by standard techniques implying cleavage and analysis of the fragments by Edman degradation and mass spectrometry. It is important to note that NMR experiments were performed on a sample of natively folded protein, and that proteolysis was performed under slightly acidic conditions to prevent scrambling of disulfide bonds. The NMR results presented here unambiguously indicate that Pi4, whether isolated from scorpion venom or obtained by chemical synthesis, adopts the standard pattern of disulfides (C1–C5, C2–C6, C3–C7, and C4–C8). Standard techniques performed on nPi4 (this work) and sPi4 (M'Barek et al. 2003) are in full agreement with this result. Initially proposed by Nilges (1995), successful assignment of S–S bonds by NMR and modeling using different methodologies has been described for several proteins (see Delepierre et al. 1999; Boisbouvier et al. 2000). Even when other experimental data are available, NMR and structure calculations offer the possibility of test-

ing the disulfide bridge pattern determined by other techniques and could be routinely used to establish the S–S bonds of proteins for which structures are to be solved. It should be noted, however, that in some cases these approaches may not produce a unique result, as was observed for the toxin MTX, for which NMR data were in full agreement with both standard and nonstandard S–S topologies (Blanc et al. 1997).

From the mutagenesis work performed on MTX (Fajloun et al. 2000b,c; Carlier et al. 2001), it has been inferred that some positions in the sequence, close to cysteines C3 and C4, are key to define whether this peptide will adopt a standard or a nonstandard S–S bridge pattern (see Fig. 1). Pi4, which has 76% sequence identity and 85% similarity with MTX, can be thought of as a natural mutant of the latter. Moreover, four (positions 4, 5, 7, and 10 in Pi4 numbering) out of the seven differences in sequence are located in a region that has been shown to be irrelevant for the MTX S–S pattern definition, and a fifth difference is a conservative one (^{28}S in MTX, ^{31}T in Pi4). The point mutation ^{14}R→^{14}Q of MTX induces a shift from the nonstandard to the standard S–S pattern (Fajloun et al. 2000c). Pi4 has also a glutamine residue at the equivalent position (^{17}Q) and displays only two other differences in sequence with MTX in the region close to C3 and C4 (^{14}R and ^{19}R in Pi4, ^{11}A and ^{16}Q in MTX, respectively). That Pi4 shows a standard S–S arrangement like the mutant ^{14}R→^{14}Q of MTX, indicates that positions 11 and 16 in MTX do not influence the S–S arrangement and that the point mutant ^{17}Q→^{17}R of Pi4 would show a nonstandard arrangement of disulfide bonds. The latter prediction, if confirmed experimentally, would further show the crucial role of the amino acid contiguous to C3 in determining the pattern of S–S adopted by MTX.

Although previous work on MTX and this work on Pi4 allow to pinpoint the positions that influence the S–S bridging pattern of MTX, a clear explanation of the factors involved is not available. Fajloun et al. (2000c) had previously hypothesized that in the absence of major structural variations between MTX and the mutant ^{15}K→^{15}Q, the substitution of a charged residue by a neutral one might modify the local electrostatic fields of the thiol group of cysteines ^{13}C (C3) and ^{19}C (C4), and thus change the reactivity of these. However, an analysis of the electrostatic potential of the S atoms in the structure of MTX, of the MTX mutant ^{15}K→^{15}Q and of Pi4, calculated by using the software DELPHI 3.0 (Accelrys; Nicholls and Honig 1991), does not corroborate this hypothesis (data not shown). A full understanding of the factors that lead to a different S–S pattern in MTX would require the study of the oxidative folding of MTX and its mutants.

Toxins of the α-KTX6 subfamily show a high level of sequence identity (47% to 76%), four disulfides, and the α/β scaffold of scorpion toxins. The structure of Pi4, obtained with 18.6 constraints per residue, is very similar to that of HsTX1 (Protein Data Bank [PDB] code 1QUZ, Cα RMSD ~ 0.9 Å for 34 residues, 50% sequence identity, 11.6, constraints/residue; Savarin et al. 1999) and Pi7 (PDB code 1QKY, Cα RMSD ~ 1.2 Å, 65% sequence identity, 9.2 constraints/residue; Delepierre et al. 1999), and seems more distant to that of Pi1 (Cα RMSD ~ 2.1 Å, 65% sequence identity, 6.0 constraints/residue; Delepierre et al. 1997), although for the latter only a low-resolution structure was obtained from a very low amount of product. The structure of MTX (PDB code 1TXM, 7.4 constraints/residue; Blanc et al. 1997), which shows a different pattern of S–S bonds, deviates from the structure of Pi4, HsTX1, and Pi7 (Cα RMSD ~ 1.8 Å, 76% sequence identity relative to Pi4). The main differences between the structures of Pi4 and MTX are located in the loop connecting the α-helix and the β-sheet, in the first strand and the region connecting both strands of the β-sheet, and in the C-terminal region. These differences may be ascribed to the two different S–S bridges between C3, C4, C7, and C8. Indeed, C4 (α-β loop), C7, and C8 (C-terminal part) are located in the regions that show higher RMSD values between the structures. In agreement with this, the structure of the mutant ^{15}K→^{15}Q of MTX (11.0 constraints/residue; Fajloun et al. 2000c), which adopts the standard S–S pattern, is more closely related to the structure of Pi4 (Cα RMSD ~ 1.4 Å) than to the structure of MTX (Cα RMSD ~ 1.9 Å). It should be mentioned that the structure of the mutant ^{33}G→^{33}A of MTX (11.3 constraints/residue; Fajloun et al. 2000c), which also shows a standard topology of disulfides, deviates from the structures of both Pi4 (Cα RMSD ~ 2.9 Å) and MTX (Cα RMSD ~ 3.4 Å), mainly because of a shift of ~50° in the angle between the α-helix and the β-sheet. It is interesting to note that there is no correlation between the level of sequence identity and the similarity of the structures of the members of the α-KTX6 subfamily. Indeed, the structure of MTX, which shows the highest level of identity with Pi4 (76% identity), is the most different from the structure of Pi4, and that of HstX1 is the most similar to the latter although HsTX1 and Pi4 only show 50% of identity. There is no correlation either between the sequence identity and the specificity of these toxins. For instance, Pi4 and Pi1 (65% identity) show a more similar pharmacological profile than do Pi4 and MTX (76% identity; Kharrat et al. 1996, 1997; Olamendi-Portugal et al. 1996, 1998; Gómez-Lagunas et al. 1997; Fajloun et al. 2000a, M'Barek et al. 2003). The latter observation, which can be expanded to other short scorpion toxins (Savarin et al. 1999), is in agreement with the now common view in the field that the differences in activity and specificity of these toxins are finely tuned by the differences in structure and in sequence among peptides that share a common fold.

Like charybdotoxin, a very well characterized scorpion toxin, Pi4 recognizes Shaker B channels with high affinity. Mutagenesis and functional studies have revealed function-

ally important residues (^{27}K, ^{29}M, ^{30}N, ^{34}R, and ^{36}Y) involved in the interaction of charybdotoxin with Shaker B (Goldstein et al. 1994; Naranjo and Miller 1996). The structures of Pi4 and charybdotoxin (PDB code 2CRD; Bontems et al. 1991) are similar, with a Cα RMSD of 1.4 Å for 33 residues. Also, the functionally important residues of charybdotoxin mentioned above, and residues ^{26}K, ^{28}I, ^{29}N, ^{33}K, and ^{35}Y of Pi4, respectively, superpose very well. In addition, it is interesting to note that the point mutations of methionine 29 into an isoleucine, or of arginine 34 to lysine in charybdotoxin—that is, into the same amino acids found in Pi4 at the equivalent position (^{28}I, ^{33}K)—do not have a significant effect in the interaction of charybdotoxin with Shaker B channels (Goldstein et al. 1994). These results strongly indicate that residues ^{26}K, ^{28}I, ^{29}N, ^{33}K, and ^{35}Y may be involved in the interaction of Pi4 with Shaker B. The well-defined structure of Pi4 here described and the high amounts of sPi4 that can be produced open the venue to study in detail the interaction of Pi4 with different types of K^+ channels and, in particular, with rat Kv 1.2 channels that Pi4 block very efficiently (M'Barek et al. 2003).

Materials and methods

Obtention of nPi4 and sPi4

Peptide nPi4 was purified from the venom of *P. imperator* scorpions. Scorpions maintained alive in the laboratory were milked for venom. The soluble part of the venom was separated by Sephadex G-50 column chromatography, followed by HPLC, essentially as described earlier (Olamendi-Portugal et al. 1998). The peptide sPi4 was obtained by solid-phase synthesis by using an automated peptide synthesizer (Model 433A, Applied Biosystems Inc.) and Fmoc (*N*-α-fluorenylmethyloxycarbonyl) chemistry. Briefly, after synthesis and removal of the resin, the mixture containing the unprotected peptide was dissolved in H_2O and lyophilized. Oxidative folding of the reduced peptide was achieved by dissolving the lyophilized mixture (~1 mM final concentration) in 0.2 M Tris-HCl buffer (pH 8.4) and incubation with gentle stirring for 72 h at 25°C. After folding, sPi4 was purified by reverse-phase semi-preparative HPLC (Perkin Elmer C18 Aquapore ODS 20 μm, 250 × 10 mm, column). The homogeneity and identity of sPi4 were established by analytical HPLC, amino acid composition analysis, Edman degradation, and mass spectrometry. The conditions used for the oxidative folding of sPi4, as well as for its synthesis and its purification, are very similar to those used for MTX and its mutants (Kharrat et al. 1996; Fajloun et al. 2000c; Carlier et al. 2001). Further details on the synthesis, folding, and purification of sPi4 are given elsewhere (M'Barek et al. 2003).

Sample preparation for NMR

Lyophilized proteins were dissolved in 5 mM CD_3COONa, 10% D_2O, (pH 4.0; NMR buffer). The concentration of nPi4 samples was 0.4 mM (40 μL volume) and 0.12 mM (150 μL) in a nanotube (Varian Inc.) or a 3 mm Shigemi (Shigemi Inc.) tube (see below), respectively. The concentration of sPi4 was 2.5 mM and 3.2 mM in the NMR buffer prepared with H_2O or D_2O, respectively.

NMR methods

Homonuclear ^{1}H experiments were acquired by using an 11.7 T Inova (Varian Inc.) spectrometer. The spectrometer was equipped with a 5-mm bore diameter pulse-field gradient probe, or, for TOCSY experiments on nPi4, with a nanoprobe rotating at 2500 Hz. Acquisition and data processing were performed by means of Vnmr 6.1C (Varian Inc.). NMRView 5.03 (Johnson and Blevins 1994) was used for spectra analysis. Experiments were run at 293, 303, or 313 K. Chemical shifts are referenced relative to the sodium salt of 4,4-dimethyl-4-silapentane sulfonate.

Two-dimensional spectra were recorded with a spectral width of 5500 Hz, with typically 16 to 32 scans per increment, 400 to 512 complex points in the indirect dimension, and a recycle delay of 2.0 or 2.2 sec. The intensity of the water signal was reduced either by presaturation during the recycle delay or by means of the Watergate pulse sequence (Piotto et al. 1992; Liu et al. 1998). Double-quantum–filtered COSY (DQF-COSY; Piantini et al. 1982; Rance et al. 1983) and purged COSY (Marion and Bax 1988) spectra were recorded with 8192 points on the direct dimension. TOCSY (Griesinger et al. 1988) spectra were acquired by using either the MLEV17 (Levitt et al. 1982; Bax and Davis 1985) sequence or adiabatic pulses when using the nanoprobe (Kupce et al. 2001) during the mixing time (70 or 80 msec). NOESY (States et al. 1982) spectra were obtained with a mixing time of 250 msec for assignment purposes, and with different mixing times (70, 100, 150, 200, and 250 msec) to obtain initial NOE buildup rates for structure calculations.

Main chain amide proton temperature coefficients were calculated from chemical shifts determined on TOCSY experiments at 293, 303, and 313 K. Exchange of sPi4 amide protons was followed by short TOCSY experiments after dissolving the lyophilized protein in the NMR buffer prepared in D_2O. Chemical shift index (CSI) prediction of secondary structure was performed with the software CSI (Wishart and Sykes 1994a,b).

Assignment of signals to peptide protons was achieved by the standard method developed by Wüthrich (1986).

Constraints for structure calculations

Structures were calculated from data of the synthetic peptide sPi4 obtained at 308 K, using NOE derived distance constraints, ϕ angle constraints issued from $^3J_{HN\text{-}H\alpha}$ coupling constants, and hydrogen bonds. Initial NOE build-up rates were calculated from the fitting of NOE volumes obtained from NOESY data in H_2O and D_2O at five mixing times: 70, 100, 150, 200, and 250 msec. Data were fit to a second-order polynomial ($ax + bx^2$). Build-up curves showing significant spin diffusion ($a \leq 0$) or poor fit were excluded. Initial rates were converted into distance constraints with ARIA 1.2 (Nilges et al. 1997; Linge et al. 2001). $^3J_{HN\text{-}H\alpha}$ coupling constants were determined from purged-COSY experiments acquired with a resolution of 1.3 Hz or, for some amide protons, from one-dimensional spectra. Coupling constants were transformed into angle constraints as follows: $-120° \pm 40°$ for $^3J_{HN\text{-}H\alpha} \geq 8.0$ Hz, $-65° \pm 40°$ for $^3J_{HN\text{-}H\alpha} \leq 5.5$ Hz. An hydrogen bond constraint was used in structure calculations only if it was present in >75% of the structures calculated without any hydrogen bond and if it was in agreement with amide temperature coefficients (≤−5 ppb/K) and exchange in D_2O data (signal present after 72 h of exchange at 303 K and pH 4.0). In addition, for the interstrand antiparallel β-sheet hydrogen bonds, these needed to be in agreement with the NOE connectivities observed for sPi4.

Assignment of NOEs and structure determination

Peaks from NOESY experiments in H_2O and D_2O NMR buffer were assigned by a combination of manual and automated methods with ARIA 1.2 (Nilges et al. 1997; Linge et al. 2001). Structures were calculated with CNS 1.1 (Brünger et al. 1998). Several cycles of ARIA using standard protocols and varying the chemical shift tolerance between 0.025 and 0.017 ppm were performed. Assignments, violations, and peaks were carefully inspected after each cycle. Calculations were performed with the standard disulfide arrangement as determined by NMR and identification of purified proteolysis peptides. For the final structures, 200 conformers were calculated with ARIA/CNS, and the 10 structures with lower total energy were minimized in an explicit-water box using the PARALLHDG 5.3 force field as described (Linge et al. 2003). Structures were analyzed and visualized with MOLMOL 2K.1 (Koradi et al. 1996).Their quality was assessed with PROCHECK 3.54 (Laskowski et al. 1993) and WHATCHECK 4.99g (Hooft et al. 1996).

Assignment of disulfide bonds by N-terminal sequencing and mass spectrometry of proteolytic peptides

A sample containing 50 μg of nPi4 was dissolved in 50 nM TRIS-HCl buffer (pH 6.8), and 10 μg of trypsin (Boehringer) was added to the sample and incubated for 8 h at 37°C. An aliquot containing 5 μg of chymotrypsin (Boehringer) was then added to the pretreated sample, and Pi4 digestion was continued overnight. The products of this double enzymatic hydrolysis were separated by HPLC on a C18 reverse column (Vydac), using a gradient from solution A (0.12% trifluoroacetic acid, TFA in water) to 40% of solution B (0.10% TFA in acetonitrile), run for 60 min. An aliquot of each peptide recovered from this HPLC separation was directly sequenced using a Beckman LF 3000 protein sequencer, with chemicals and protocols established by the company. Another sample from the same HPLC fractions was analyzed by mass spectrometry using a Finnigan LCQ^{Duo} ion-trap mass spectrometer.

Sf9 cells culture and Shaker B expression

Insect Sf9 cells were kept in culture at 27°C in Grace media (GIBCO). Cells were infected (multiplicity of infection of 10) by means of a recombinant baculovirus containing the cDNA of Shaker B channels as described (Olamendi-Portugal et al. 1998). Electrophysiological experiments were run 48 h after cell infection.

Electrophysiological recordings

Macroscopic currents were recorded under whole-cell patch clamp with a Multiclamp 700A (Axon Instruments). The currents were filtered at 5 KHz and sampled at a rate of 100 μsec/point with a Digidata 1322A interface (Axon Instruments). Electrodes of Borosilicate glass (KIMAX 51) were pulled to a 1 to 1.5 MΩ resistance. Eighty percent of the series resistance was compensated. The holding potential was −90 mV. Activating pulses were applied every 20 sec to allow complete recovery from inactivation. The internal solution was (in mM) 90 KF, 30 KCl, 2 $MgCl_2$, 10 EGTA, and 10 HEPES-K buffer (pH 7.2), whereas the external solution was (in mM) 145 NaCl, 10 $CaCl_2$, and 10 HEPES-Na buffer (pH 7.2).

Electronic supplemental material

Two tables showing chemical shifts of synthetic sPi4 in H_2O (Pi4cswat.pdf) and D_2O (Pi4csdeu.pdf), a table with amide temperature coefficients of sPi4 and nPi4 (Pi4tmcoe.pdf), and a figure with structure backbone RMSDs and distance constraints used for structure calculations on a per residue basis (ConsRms.pdf). PDF files were generated on a Macintosh platform.

Acknowledgments

We thank Dr. Amor Mosbah for kindly providing the coordinates of the MTX mutants. The NMR spectrometer was funded by the Région Ile de France and the Institut Pasteur.

The publication costs of this article were defrayed in part by payment of page charges. This article must therefore be hereby marked "advertisement" in accordance with 18 USC section 1734 solely to indicate this fact.

Accession numbers

The atomic coordinates of the structure of Pi4 have been deposited with the RCBS Protein Data Bank (PDB code 1N8M); chemical shift data have been deposited with the BioMagResBank (accession no. 5676).

References

Batista, C.V.F., Gómez-Lagunas, F., Lucas, S., and Possani, L.D. 2000. Tc1, from *Tityus cambridgei*, is the first member of a new subfamily of scorpion toxins that blocks K^+-channels. *FEBS Lett.* **486:** 117–120.

Bax, A. and Davis, D.G. 1985. MLEV-17–based two-dimensional homonuclear magnetization transfer spectroscopy. *J. Magn. Reson.* **65:** 355–360.

Blanc, E., Sabatier, J.M., Kharrat, R., Meunier, S., El Ayeb, M., Van Rietschoten, J., and Darbon, H. 1997. Solution structure of maurotoxin, a scorpion toxin from *Scorpio maurus*, with high affinity for voltage-gated potassium channels. *Protein* **29:** 321–333.

Boisbouvier, J., Blackledge, M., Sollier, A., and Marion, D. 2000. Simultaneous determination of disulphide bridge topology and three-dimensional structure using ambiguous intersulphur distance restraints: Possibilities and limitations. *J. Biomol. NMR* **16:** 197–208.

Bontems, F., Roumestand, C., Gilquin, B., Ménez, A., and Toma, F. 1991. Refined structure of charybdotoxin: Common motifs in scorpion toxins and insects defensins. *Science* **253:** 1521–1523.

Brünger, A.T., Adams, P.D., Clore, G.M., DeLano, W.L., Gros, P., Grosse-Kunstleve, R.W., Jiang, J.S., Kuszewski, J., Nilges, M., Pannu, N.S., et al. 1998. Crystallography and NMR system: A new software suite for macromolecular structure determination. *Acta Cryst. D* **54:** 905–921.

Carlier, E., Fajloun, Z., Mansuelle, P., Fathallah, M., Mosbah, A., Oughideni, R., Sandoz, G., Di Luccio, E., Geib, S., Regaya, I., et al. 2001. Disulfide bridge reorganization induced by proline mutations in maurotoxin. *FEBS Lett.* **489:** 202–207.

Corona, M., Gurrola, G.B., Merino, E., Restano Cassulini, R., Valdez-Cruz, N.A., García, B., Ramírez-Domínguez, M.E., Coronas, F.I.V., Zamudio, F.Z., Wanke, E., et al. 2002. A large number of novel Ergtoxin-like genes and ERG K^+-channels blocking peptides from scorpions of the genus *Centruroides*. *FEBS Lett.* **532:** 121–126.

Delepierre, M., Prochnicka-Chalufour, A., and Possani, L.D. 1997. A novel potassium channel blocking toxin from the scorpion *Pandinus imperator*: A ^1H NMR analysis using a nano-nmr probe. *Biochemistry* **36:** 2649–2658.

Delepierre, M., Prochnicka-Chalufour, A., Boisbouvier, J., and Possani, L.D. 1999. Pi7, an orphan peptide from the scorpion *Pandinus imperator*: A

^{1}H-NMR analysis using a nano-NMR probe. *Biochemistry* **38:** 16756–16765.

Devaux, C., Knibiehler, M., Defendini, M.L., Mabrouk, K., Rochat, H., Van Rietschoten, J., Baty, D., and Granier, C. 1995. Recombinant and chemical derivatives of apamin: Implication of post-transcriptional C-terminal amidation of apamin in biological activity. *Eur. J. Biochem.* **231:** 544–550.

Fajloun, Z., Carlier, E., Lecomte, C., Geib, S., Di Luccio, E., Bichet, D., Mabrouk, K., Rochat, H., De Waard, M., and Sabatier, J.M. 2000a. Chemical synthesis and characterization of Pi1, a scorpion toxin from *Pandinus imperator* active on K^+ channels. *Eur. J. Biochem.* **267:** 5149–5155.

Fajloun, Z., Ferrat, G., Carlier, E., Fathallah, M., Lecomte, C., Sandoz, G., di Luccio, E., Mabrouk, K., Legros, C., Darbon, H., et al. 2000b. Synthesis, ^{1}H NMR structure, and activity of a three-disulfide-bridged maurotoxin analog designed to restore the consensus motif of scorpion toxins. *J. Biol. Chem.* **275:** 13605–13612.

Fajloun, Z., Mosbah, A., Carlier, E., Mansuelle, P., Sandoz, G., Fathallah, M., di Luccio, E., Devaux, C., Rochat, H., Darbon, H., et al. 2000c. Maurotoxin versus Pi1/HsTx1 scorpion toxins: Toward new insights in the understanding of their distinct disulfide bridge patterns. *J. Biol. Chem.* **275:** 39394–39402.

Goldstein, S.A., Pheasant, D.J., and Miller, C. 1994. The charybdotoxin receptor of a Shaker K^+ channel: Peptide and channel residues mediating molecular recognition. *Neuron* **12:** 1377–1388.

Gómez-Lagunas, F., Olamendi-Portugal, T., and Possani, L.D. 1997. Block of Shaker B K^+ channels by Pi1, a novel class of scorpion toxin. *FEBS Lett.* **400:** 197–200.

Griesinger, C., Otting, G., Wüthrich, K., and Ernst, R.R. 1988. Clean Tocsy for ^{1}H spin system identification in macromolecules. *J. Am. Chem. Soc.* **110:** 7870–7872.

Hooft, R.W., Vriend, G., Sander, C., and Abola, E.E. 1996. Errors in protein structures. *Nature* **381:** 272.

Johnson, B.A. and Blevins, R.A. 1994. NMRView: A computer program for the visualisation and analysis of NMR data. *J. Biomol. NMR* **4:** 603–614.

Kharrat, R., Mabrouk, K., Crest, M., Darbon, H., Oughideni, R., Martin-Eauclaire, M.F., Jacquet, G., El Ayeb, M., Van Rietschoten, J., Rochat, H., et al. 1996. Chemical synthesis and characterization of maurotoxin, a short scorpion toxin with four disulfide bridges that acts on K^+ channels. *Eur. J. Biochem.* **242:** 491–498.

Kharrat, R., Mansuelle, P., Sampieri, F., Crest, M., Oughideni, R., Van Rietschoten, J., Martin-Eauclaire, M.F., Rochat, H., and El Ayeb, M. 1997. Maurotoxin, a four disulfide bridge toxin from *Scorpio maurus* venom: Purification, structure and action on potassium channels. *FEBS Lett.* **406:** 284–290.

Koradi, R., Billeter, M., and Wüthrich, K. 1996. MOLMOL: A program for display and analysis of macromolecular structures. *J. Mol. Graphics* **14:** 51–55.

Kupce, E., Keifer, P.A., and Delepierre, M. 2001. Adiabatic TOCSY MAS in liquids. *J. Magn. Reson.* **148:** 115–120.

Laskowski, R.A., MacArthur, M.W., Moss, D.S., and Thornton, J.M. 1993. PROCHECK: A program to check the stereochemical quality of protein structures. *J. Appl. Crystallogr.* **26:** 283–291.

Lebrun, B., Romi-Lebrun, R., Martin-Eauclaire, M.F., Yasuda, A., Ishiguro, M., Oyama, Y., Pongs, O., and Nakajima, T. 1997. A four-disulphide–bridged toxin, with high affinity towards voltage-gated K^+ channels, isolated from *Heterometrus spinnifer* (Scorpionidae) venom. *Biochem. J.* **328:** 321–327.

Levitt, M.H., Freeman, R., and Frenkiel, T. 1982. Broadband heteronuclear decoupling. *J. Magn. Reson.* **47:** 328–330.

Linge, J.P., O'Donoghue, S.I., and Nilges, M. 2001. Automated assignment of ambiguous nuclear Overhauser effects with ARIA. *Methods Enzymol.* **339:** 71–90.

Linge, J.P., Habeck, M., Rieping, M., and Nilges, M. 2003. Refinement of protein structures in explicit solvent. *Protein* **50:** 496–506.

Liu, M.L., Mao, X.-A., Ye, C.H., Huang, H., Nicholson, J.K., and Lindon, J.C. 1998. Improved WATERGATE pulse sequences for solvent suppression in NMR spectroscopy. *J. Magn. Reson.* **132:** 125–129.

Marion, D. and Bax, A. 1988. P.COSY, a sensitive alternative for double-quantum–filtered COSY. *J. Magn. Reson.* **80:** 528–533.

M'Barek, S., Mosbah, A., Sandoz, G., Fajloun, Z., Olamendi-Portugal, T., Rochat, H., Sampieri, F., Guijarro, J.I., Mansuelle, P., Delepierre, M., et al. 2003. Synthesis and characterization of Pi4, a scorpion toxin from *Pandinus imperator* that acts on K+ channels. *Eur. J. Biochem.* (in press)

Naranjo, D. and Miller, C. 1996. A strongly interacting pair of residues on the contact surface of charybdotoxin and a Shaker K^+. *Neuron* **16:** 123–130.

Nicholls, A. and Honig, B. 1991. A rapid finite difference algorithm, utilizing succesive over-relaxation to solve the Poisson-Boltzmann equation. *J. Comput. Chem.* **12:** 435–445.

Nilges, M. 1995. Calculation of protein structures with ambiguous distance restraints: Automated assignment of ambiguous NOE crosspeaks and disulphide connectivities. *J. Mol. Biol.* **245:** 645–660.

Nilges, M., Macias, M.J., O'Donoghue, S.I., and Oschkinat, H. 1997. Automated NOESY interpretation with ambiguous distance restraints: The refined NMR solution structure of the pleckstrin homology domain from β-spectrin. *J. Mol. Biol.* **269:** 408–422.

Olamendi-Portugal, T., Gómez-Lagunas, F., Gurrola, G.B., and Possani, L.D. 1996. A novel structural class of K^+-channel blocking toxin from the scorpion *Pandinus imperator*. *Biochem. J.* **315:** 977–981.

———. 1998. Two similar peptides from the venom of the scorpion *Pandinus imperator*, one highly effective blocker and the other inactive on K^+ channels. *Toxicon* **36:** 759–770.

Piantini, U., Sørensen, O.W., and Ernst, R.R. 1982. Multiple quantum filters for elucidating NMR coupling networks. *J. Am. Chem. Soc.* **104:** 6800–6801.

Piotto, M., Saudek, V., and Sklenár, V. 1992. Gradient-tailored excitation for single-quantum NMR spectroscopy of aqueous solutions. *J. Biomol. NMR* **2:** 661–665.

Rance, M., Sørensen, O.W., Bodenhausen, G., Wagner, G., Ernst, R.R., and Wüthrich, K. 1983. Improved spectral resolution in COSY ^{1}H NMR spectra of proteins via double quantum filtering. *Biochem. Biophys. Res. Comm.* **117:** 479–485.

Sabatier, J.M., Zerrouk, H., Darbon, H., Mabrouk, K., Benslimane, A., Rochat, H., Martin-Eauclaire, M.F., and Van Rietschoten, J. 1993. P05, a new leiurotoxin I–like scorpion toxin: Synthesis and structure-activity relationships of the α-amidated analog, a ligand of Ca^{2+}-activated K^+ channels with increased affinity. *Biochemistry* **32:** 2763–2770.

Savarin, P., Romi-Lebrun, R., Zinn-Justin, S., Lebrun, B., Nakajima, T., Gilquin, B., and Menez, A. 1999. Structural and functional consequences of the presence of a fourth disulfide bridge in the scorpion short toxins: Solution structure of the potassium channel inhibitor HsTX1. *Protein Sci.* **8:** 2672–2685.

States, D.J., Haberkorn, R.A., and Ruben, D.J. 1982. A two dimensional nuclear Overhauser experiment with pure absorption phase in four quadrants. *J. Magn. Reson.* **48:** 286–292.

Thompson, J.D., Higgins, D.G., and Gibson, T.J. 1994. CLUSTAL W: Improving the sensitivity of progressive multiple sequence alignment through sequence weighting, positions-specific gap penalties and weight matrix choice. *Nucleic Acids Res.* **22:** 4673–4680.

Wishart, D.S. and Sykes, B.D. 1994a. The ^{13}C chemical-shift index: A simple method for the identification of protein secondary structure using ^{13}C chemical-shift data. *J. Biomol. NMR* **4:** 171–180.

———. 1994b. Chemical shifts as a tool for structure determination. *Methods Enzymol.* **239:** 363–392.

Wüthrich, K. 1986. in NMR of proteins and nucleic acids. John Wiley & Sons, New York.